MiR-4792 regulates inflammatory responses in *Cryptococcus neoformans* infected microglia

Jianghan Chen (chenjianghan@smmu.edu.cn)
Changzheng Hospital
Guotai Yao
Changzheng Hospital
Xiaoli Wang
Changzheng Hospital
Qing Hou
Changzheng Hospital
Rui Gao
Changzheng Hospital
Yilin Wang
Changzheng Hospital
Liang Teng
Changzheng Hospital
Wenting Lin
Changzheng Hospital
Yan Wang
Changzheng Hospital
Zhongzhi Wang
Changzheng Hospital
Yi Jin
Changzheng Hospital

Research article

Keywords: miR-4792, EGFR; MAPK, inflammatory cytokines, cryptococcus neoformans

Posted Date: March 17th, 2020

DOI: https://doi.org/10.21203/rs.3.rs-17417/v1

Abstract

Background: Investigating the factors that influence inflammatory response of microglial cells is important to understand the pathogenesis of cryptococcal meningitis (CM). MicroRNA (miRNA) have been shown to play an important role in inducing host defenses and activating immune response in the process of microbial infection; however, the regulatory mechanisms of miRNAs in cryptococcal meningitis are poorly defined. In our previous analysis, we assessed the miRNA profiles of BV2 cells following *Cryptococcus neoformans (C. neoformans)* infection. In this study, we characterized the expression of miR-4792 in CM patients to further our understanding of the host response to pathogen infections.

Results: miR-4792 was downregulated in BV2 cells infected with *C. neoformans* while its target gene EGFR was upregulated. Infected cells with up-regulated miR-4792 exhibited decreased EGFR expression, reduced MAPK signaling and a decreased secretion of inflammatory cytokines. Following antifungal treatment in cryptococcal meningitis patients, the levels of miR-4792 in the CSF significantly increased, while the expression of EGFR significantly decreased.

Conclusion: This study identified that miR-4792 and its target EGFR regulate the secretion of inflammatory cytokines in *C. neoformans* infected BV2 cells. This furthers our knowledge of the host immune responses to fungal infections in the CNS.

Background

Cryptococcal meningitis (CM) causes mortality rates of 15% in acquired immunodeficiency (AIDS) patients, accounting for approximately 181,100 deaths per year. China and other developing countries have observed a higher impact of CM infection in non-HIV AIDS hosts with no known risk of susceptibility [1–2]. C. neoformans is the major cause of CM due to its tropism for neuronal tissue. Infection is initiated in the lungs following the inhalation of fungal spores and spreads to the brain of immunosuppressed individuals.

Microglia are macrophages within the central nervous system (CNS) that participate in the immunosurveillance of C. neoformans. The efficiency of the immune response dictates the outcome of C. neoformans infection, producing a disseminated disease or state of latency. The CNS is immune-privileged and isolated from other peripheral organs due to separation by the blood–brain barrier (BBB). Microglial activation enhances innate immune response, enhancing the phagocytosis of invasive bacteria or fungi, thus protecting neuronal cells [3–4]. Assessment of the relationship between macrophage, innate immunity and C. neoformans can enhance our understanding of CM pathogenesis.

miRNAs are highly conserved small non-coding RNAs 18–22 nucleotides in length [5]. miRNAs regulate gene expression through binding to the 3'UTR of miRNAs that lead to a loss of gene expression through mRNA degradation or through preventing translation. Recently, a role for miRNAs in the immune response to fungal exposure has been documented. miR-21, miR-146, miR-132, miR-155, and the let-7 family

regulate inflammatory responses following exposure to bacterial pathogens. The miRNA response to fungal exposure is comparable to that of inflammatory and allergic responses [6–11].

Approximately 50% of cryptococcal meningitis patients die within a year of infection due to a lack of successful therapy [12]. In the absence of effective anti-fungal agents, the immune response to fungal infection requires further understanding. The molecular mechanisms underlying these responses remain poorly defined for a range of fungal species. In this regard, knowledge of the miRNA response to pathogen infections can guide novel and effective approaches to antifungal therapeutics.

Results

miR-4792 and EGFR expression in BV2 cells induced by C. neoformans (WM148)

It has been shown that miR-4792 is downregulated in nasopharyngeal carcinoma, uterine leiomyoma, during submucosal fibrosis and in glioblastoma-infiltrating CD14 + cells. In contrast, miR-4792 is upregulated in glioma microvesicles [13–17]. Our previous studies have shown that the expression of miR-4792 increases in THP-1 cells infected with C.neoformans (WM148) (Fig. 1a) [6]. To further study the expression of miR-4792 in microglia, BV2 cells were treated with WM148 for 0, 3, 6 and 9 and 12 h and qRT-PCR was performed to detect miR-4792 expression. We found that the expression of miR-4792 decreased over time, reaching its lowest after 6 h (Fig. 1b), while the expression of EGFR gradually increased, peaking at 6 h (Fig. 1c). ELISA assays showed that the inflammatory factors TNF-α and IL-6 secreted by microglia gradually increased over time, while IL-1β levels showed no obvious changes (Fig. 1d).

EGFR is targeted by miR-4792.

To further define the molecular mechanisms governing the regulatory effects of miR-4792, we performed targeted bioinformatics to investigate novel miR-4792 targets using MIRADA and target scan. These analyses revealed EGFR as miRNA target, the sequence of which was assumed to be in the 3’UTR (Fig. 2a). We additionally performed western blot analysis to assess the expression of the Phosphorylation of EGFR (pEGFR) in BV2 cells. We found that miR-4792 overexpression significantly reduced pEGFR levels, and dual luciferase assays confirmed EGFR as a direct target of miR-4792 (Fig. 2b). The exogenous overexpression of miR-4792 significantly inhibited WT EGFR 3’-UTR activity, but had minimal effect on mutant EGFR 3’UTR sequence (Fig. 2c). These data strongly implicate EGFR as a direct target for miR-4792.

EGFR blockade inhibits WM148 induced microglia activation

Microglia regulate the innate immune responses of the CNS [18, 19]. Given that microglia are responsible for pro-inflammatory cytokine production [20], we investigated the effects of WM148 on microglia induction. Western blot analysis was performed to assess the expression of the cell surface molecule CD11b, considered a phenotypic marker of microglial activation [21]. The data showed that, after 6 h of

WM148 treatment, higher levels of CD11b expression and EGFR activation (evident through the enhanced levels of pEGFR) occurred in treated BV2 cells (Fig. 3a). In contrast, 24 h treatment with EGFR inhibitor (AG1478) led to a loss of CD11b and pEGFR expression (Fig. 3b) confirmed by western blot analysis. Interestingly miR-4792 expression inversely correlated with EGFR levels, further highlighting EGFR as a miR-4792 target (Fig. 3c).

Inhibiting EGFR prevents MAPK kinase mediated cytokine production in BV2 cells

Activated microglia stimulate neuronal inflammation and enhance the levels of proinflammatory cytokines including IL-1β and TNF-α in the CNS [22]. Extracellular signal-regulated kinases (Erk1/2), c-Jun terminal kinase (JNK) and p38 MAPK are key cellular signaling cascades MAPKs are known to enhance the production and secretion of cytokines [23–25]. For example, MAPK signaling promotes the LPS-induced synthesis of IL-1β and TNF-α [26]. MAPK is also stimulated following EGFR activation [27, 28]. Consistent with previous findings, we found that AG1478 treatment inhibited MAPK phosphorylation leading to a loss of ERK1/2, p38MAPK and JNK activation in WM148 treated BV2 cells, while no significant differences in p-JNK levels were observed (Fig. 4a). Similarly, AG1478 treatment inhibited both IL-1β and TNF-α production in WM148 infected BV2 cells (Fig. 4b). We simultaneously assessed the secretion of other inflammatory factors in WM148 infected BV2 cells. The results showed that IL-1α, IL-12, Eotaxin, GM-CSF, MCP-1/CCL2 levels decreased after AG1478 treatment compared to the control group (Fig. 4c), but the differences were not significant.

miR-4792 regulates the EGFR/MAPK axis in BV2 cells

We next investigated the effects of the miR-4792-mediated regulation of EGFR on ERK1/2, JNK and P38MAPK signaling in BV2 cells infected with WM148. As shown in Fig. 2b and Fig. 5a, the levels of active pEGFR and p-ERK1/2, p-p38 and p-JNK decreased in the presence of miR-4792 mimics compared to the WM148 group, and the levels of the inflammatory cytokines IL-1β and TNF-α also decreased (Fig. 5b). While there is no significant different when BV2 cells were treated with miR-4792 inhibitors. All findings were confirmed by qRT-PCR analysis in which the expression of miR-4792 significantly increased, while EGFR expression decreased following the transfection of miR-4792 mimics for 24 h. The opposite phenotype was observed for miR-4792 inhibitors (Fig. 5c). We additionally found that active pEGFR levels were highly expressed when miR-4792 expressed lowly following WM148 stimulation (Fig. 1). Furthermore, we assessed the secretion of other inflammatory factors in WM148 infected BV2 cells, and found that the levels of pro-inflammatory factors including IL-1α, IL-12, Eotaxin, GM-CSF, MCP-1/CCL2 decreased after treatment with miR-4792 mimics for 24 h (Fig. 5d). Taken together, these data highlight that in BV2 cells, miR-4792 regulates EGFR/MAPK signaling following WM148 infection and partially alleviates MAPK-mediated inflammatory responses therefore affect the production of pro-inflammatory factors following WM148 infection.

Expression of miR-4792 in patients with CM before and after treatment

We collected CSF from patients with CM before and after regular antifungal treatment. The results showed that the expression of miR-4792 in CSF significantly increased after treatment (Fig. 6a). Receiver operating characteristics (ROC) curve analysis showed the areas under curves (AUCs) of 0.75 (95% CI, 0.54–0.96) (Fig. 6b). We also found the expression of EGFR in CSF significantly decreased after treatment (Fig. 6c). Receiver operating characteristics (ROC) curve analysis showed the areas under curves (AUCs) of 0.79 (95% CI, 0.6–0.98) (Fig. 6d). These data confirmed the reciprocal relationship between miR-4792 and EGFR in vivo setting of fungal infection and showed that the CSF miR-4792 and EGFR might be served as an useful biomarker for judging the effort of the treatment of CM patients.

Discussion

Cryptococcal meningitis (CM) is 100% fatal if not immediately treated and predominates in immunocompromised individuals [29]. CM diagnostics have rapidly improved over the last 10 years due to advancements in point-of-care testing that is highly specific, sensitive, accurate and capable of data production within 10 min of test initiation [30, 31]. Despite diagnostic advances, the discovery of effective anti-fungal agents has stalled. In this study, we present data that has relevance for the discovery of immunomodulatory therapies that provides a perspective to improve the immune modulation to fungal infection, providing hope for future CM treatment regimens.

MicroRNAs protect the host from infection by regulating key genes involved in host immune defenses amongst different phenotypes of macrophages and immune response [32, 33]. In vitro, macrophage phagocytosis directly correlates with the clinical outcome [34, 35]. Following C. neoformans exposure in human monocytic THP-1 cells, miR-146a is upregulated and inhibits NF-κB activation and inflammatory cytokine release [6]. MiRNAs act in concert to induce host defenses and are frequently dysregulated in an array of disease models, including the exposure to fungal pathogens. As such, miRNAs serve as novel biomarkers for fungal infections. By screening differentially expressed microRNAs in C. neoformans infection and studying their interactions with microglia, we found that miR-4792 represents a potential immunomodulatory therapy of cryptococcosis that can improve the design of antifungal drugs and may hold value as a biomarker for C. neoformans exposure.

In BV2 cells, exposure to WM148 led to a significant upregulation of IL-1β, TNF-α, and IL-6. Pro-inflammatory cytokines are key mediators of neuroinflammation in many CNS pathologies, highlighting the ability of C. neoformans to induce a neuroinflammatory phenotype. BV2 cells are RAF/Myc immortalized murine neonatal microglia models and act as surrogates for primary microglia [36]. The suitability of BV2 microglia as an alternative model system has been established previously [36, 37]. These in vitro data further highlight the inflammatory responses induced by C. neoformans.

Microglia have been heavily implicated in neuroinflammation in response to a broad range of intrinsic or external stimuli [38]. Microglia are key effector cells in the host defenses to microbial infections and act as antigen presenting cells that can produce active substances that promote inflammatory cell death [39, 40]. Following C. neoformans exposure, microglia produce TNF-α, IL-1β and IL-6 to upregulate MHC Class

II and CD11c [41, 42]. Moreover, microglia can phagocytose C. neoformans and upregulate iNOS with anti-fungal effects which is dependent on GPR43 expression [43–46]. Despite the phagocytic capabilities of microglia, they are unable to destroy yeast cells and remain susceptible to latent intracellular infections [46, 47]. Microglia are also activated in response to injury in which cell-surface CD11b is a typical phenotypic marker [48]. Microglia continually survey the microenvironment for noxious agents and injurious processes, and respond to extracellular signals, clear debris and toxic substances, and secret trophic factors, providing neuroprotection following central nervous system (CNS) injury. Increasing evidence implicates microglia activation as a major cause of CNS inflammation, the suppression of which reduces tissue damage and morphological alterations [49–51]. This highlights microglia as critical for analysis in C. neoformans infection.

In this study, we confirm a role for EGFR/MAPK signaling in WM148 mediated inflammation in the CNS. EGFR is expressed in astrocytes, neurons oligodendrocytes and microglia [52, 53]. The inhibition of EGFR/MAPK signaling prevents microglial inflammatory responses, through dampening down Ras-Raf-MAPK signaling [54]. MAPK activation is essential for the production of inflammatory cytokines, including IL-1β, TNF-α and IL-6 and regulates cell survival, differentiation and proliferation through its effects on gene expression [23, 55]. Oral epithelial cells infected with Candida albicans activate three MAPK subfamilies and enhance the production of inflammatory mediators. Sporothrix schenckii yeast induces robust activation of JNK, ERK1/2 and p38 MAPK in dendritic cells, which is related to IL-6 and TNF-α secretion. Recent study demonstrated that miR-4792 participates in the apoptotic induction of A549 cells by RTHF via MAPK pathway and determines the potential apoptotic mechanism[56]. In this study, we found that miR-4792 mimics/inhibitors did not significantly influence EGFR expression at the transcription level, suggestive of translational regulation. This study found that the inhibition of EGFR leads to the inhibition of downstream MAPK signaling, preventing microglial activation and inflammatory cytokine production. Taken together, these data highlight the importance of EGFR and its effect on MAPK signaling and pro-inflammatory factors during the microglial inflammatory response to C. neoformans.

The exposure to dangerous pathogenic fungal infections poses a risk to human health. Enhancing our understanding of the mechanisms governing the host innate immune response to pathogenic infections can advance the discovery of anti-fungal agents. Previous studies have solely focused on the end-points of the host response to fungal exposure but the specific molecular mechanisms underlying these responses differ for fungal species. Although an array of studies have investigated the pulmonary immunological response following both chronic and acute exposure to lethal fungal spores, the miRNAs that mediate these responses/deficiencies are poorly characterized. In this study, using an up-to-date models, and the assessment of miR-4792 and EGFR in clinical samples, we specifically analyzed the role of miR-4792 and EGFR in the host immune response to fungal exposure, Our data provide a platform for the future development of anti-fungal immune therapeutic regimens and permit the identification of at-risk populations, enabling targeted treatments to those deemed most at risk and can provide a new way to judge the effort of the treatment of CM patients. However, some limitations exist, for example, human primary microglia are difficult to culture in vitro, and so BV2 cells were used as an alternative. As miRNAs are highly conserved, the results can guide future human assessments. Further studies on the role of miR-

4792 in cryptococcal meningitis animal models are now required through the intramedullary injection of miR-4792 liposomes or exosomes.

Conclusions

In summary, both our in vivo and in vitro data highlight how miR-4792 regulates microglial activation and neuroinflammation in response to fungal infection. We further highlight the role of the EGFR/MAPK axis in mediating these responses.

Materials And Methods

Patients

CSF samples were obtained from 11 patients with cryptococcal meningitis (7 males and 4 females; age range 16-62 years, mean 45 years old, all HIV(-). CSF were collected before and after effective antifungal therapy at our local hospital).All of the patients fulfilled the criteria of the Infectious Diseases Society of America (IDSA). All protocols were approved by the ethics committee of our institute and were performed according to the declaration of Helsinki guidelines.

Cell Culture

Given the limited availability of primary cultures, BV2 cells were used as representative immortalized microglia cell lines due to their known similarities to glial cells [57,58]. Cells were cultured under standard tissue culture conditions in complete DMEM (Gibco) containing 10 FBS and 1 % penicillin/streptomycin. The cell densities were never allowed to exceed 5×10^5 cells/cm^2.

Induction of BV2 cells

Cells were seeded into 6-well plates and stimulated with *C. neoformans* (WM148) for 6 h to create an inflammatory environment. Cells were then treated with the AG1478, miR-4792 inhibitor, miR-4792 inhibitor NC, miR-4792 mimics and miR-4792 mimics NC for 24 h. Untreated BV2 cells served as negative controls.

Western blot analysis

For western blot (WB) analysis, BV2 cells were harvested in lysis buffer and total cell proteins were resolved by SDS-PAGE electrophoresis. Proteins were transferred to PVDF membranes which were blocked and labeled with the appropriate primary antibodies overnight at 4°C. Membranes were then washed and labeled with HRP-conjugated secondary antibodies for 1 h. ECL was used to visualize protein bands. Membranes were exposed on X-ray films, developed and imaged.

Quantification of cytokines

WM148 infected BV2 cells were treated AG1478 (100 ng/mL) for 6 h, and miR-4792 mimics and inhibitors for 24 h. Post-treatments, cell culture supernatants were collected and the levels of TNF-α, IL-1β and IL-6 were measured by ELISA according to the manufacturer's instructions. IL-1α, IL-12, Eotaxin, GM-CSF, MCP-1/CCL2 were quantified using Mouse Multi-Analyte Kits (Bio-Plex Suspension Array System; Bio-Rad, Hercules, CA, USA) according to the manufacturer's instructions. Antibody arrays were performed by Wayen Biotechnology (Shanghai, China) according to established protocols. Briefly, 50μL of antibody-conjugated beads were added to the assay plates to which 50 μL of tissue lysates, standards, and blank controls were added in the dark at room temperature (RT) with shaking at 850 rpm for 2h. After washing, 50 μL of biotinylated antibodies were added to the plate in the dark at RT with shaking at 850 rpm for 1h. Plates were then washed and 50 μL of streptavidin-phycoerythrin (PE) was added in the dark at RT with shaking at 850 rpm for 30 min. Plates were then washed and read using a Bio-Plex MAGPIX Multiplex Reader (Bio-Rad, Hercules, CA, USA). Bio-Plex Manager 6.0 software was used for data acquisition and analysis.

qRT-PCR and ELISA analysis

Cells (1×10^5 cells/cm^2) were seeded onto coverslips and treated with AG1478 for 24 h following WM148 induction. The cell culture media form each sample was assessed by ELISA and RNA was extracted at various timepoints post-harvesting.

For qRT-PCR analysis, total mRNA was extracted using MagExtractor and 1 μg of mRNA was subject to RT using ReverTra Ace (Toyobo). PCRs were performed using hot-star PCR mixes from 1 μl of cDNA template in a reaction volume of 25 μl. Successful PCRs were confirmed following gel electrophoresis visualized on a Gene Genius Bio-Imaging system (Syngene). Target gene expression was calculated relative to β-actin and values were normalized to untreated controls.

Transient overexpression studies

Cells at a density of 2×10^5 cells/plate were transfected with miR-4792 mimics (50 nM), mimics control (50 nM), the miR-4792 inhibitor (100 nM) and inhibitor control (100 nM) using riboFECTTMCP Reagent (RiboBio) as per the manufacturer's instructions. Briefly, 5ul of the miRNAs mimics or 10ul of the miRNAs inhibitor was diluted with 120 ul riboFECTTM CP buffer at 37°C for 10 min. Diluents were mixed with 12 ul of riboFECTTM CP Reagent and incubated for 15 min at 37°C. RiboFECTTM CP-miRNA mixtures were then added to cells with 1 mL of DMEM and incubated at 37°C for 24 h.

Luciferase reporter assay

BV2 cells were exogenously transfected with either miR-controls and miR-4792 mimics in combination with WT and mut 3'UTR EGFR. Forty-eight hours post-transfection, dual-luciferase reporter assays were performed to monitor Firefly and Renilla luciferase activity, as per the manufacturers protocols (Promega).

Statistical analysis

Groups differences were compared through a student t-test or one way ANOVA for multiple comparisons to control groups. Data are shown as the mean ± SD. Data were analyzed using SPSS software 19.0. Experiments were performed on at least three independent occasions. P-values < 0.05 were considered statistically significant.

Abbreviations

CM: Cryptococcal meningitis; miRNA: microRNA; CNS: central nervous system; AIDS: acquired immunodeficiency; BBB: blood–brain barrier; CSF: cerebrospinal fluid; Erk: Extracellular signal-regulated kinases; JNK: c-Jun terminal kinase. ANOVA: Analysis of variance; AUC: areas under curves; ROC: Receiver operating characteristics; CI, confidence interval; qRT-PCR: Reverse transcription quantitative PCR;

Declarations

Acknowledgements

We thank the National Natural Science Foundation of China for funding this research.

Authors' contributions

JHC and ZZW conceived the study, supervised the experiments and secured funding. GTY and XLW conceived and carried out all experiments, data analysis, wrote the manuscript and manuscript writing. YJ performed the experiments and edited the manuscript. QH, RG, YLW performed the experiments and analyzed data. LT participated in the study design, supervised the experiments. YW and WTL performed data analysis .All authors have read and approved the final manuscript.

Funding

This study was supported by the National Natural Science Foundation of China（NSFC） (Grant No: 81772158). The funding source had no role in the study design, analysis, collection, data

interpretation and manuscript writing.

Availability of data and materials

All data generated or analysed during this study are included in this published article.

Ethics approval and consent to participate

This study was approved by the Ethics Review Committee of Changzheng Hospital, China. With written permission from the patients, the CSF samples were obtained from 11 patients with cryptococcal meningitis.

Consent for publication

Not applicable.

Competing interests

The authors declare that they have no competing interests.

Author details

[1]Department of Dermatology, Changzheng Hospital, Second Military Medical University, No. 415 Fengyang Road, Shanghai, 200003, China

References

1. Pappas PG. Cryptococcal infections in non-HIV-infected patients. Trans Am Clin Climatol Assoc. 2013;124:61–79.
2. Rajasingham R, Smith RM, Park BJ, Jarvis JN, Govender NP, Chiller TM, et al. Global burden of disease of HIV-associated cryptococcal meningitis: an updated analysis. Lancet Infect Dis. 2017;17:873–881.
3. Ribes S, Ebert S, Regen T, Agarwal A, Tauber SC, Czesnik D, et al. Toll-like receptor stimulation enhances phagocytosis and intracellular killing of nonencapsulated and encapsulated Streptococcus pneumoniae by murine microglia. Infect Immun. 2010;78:865–871.
4. Redlich S, Ribes S, Schütze S, Eiffert H, Nau R. Toll-like receptor stimulation increases phagocytosis of *Cryptococcus neoformans* by microglial cells. J Neuroinflammation. 2013;10:71.

5. Gebert L, MacRae IJ. Regulation of microRNA function in animals. Nat Rev Mol Cell Biol. 2019;20;21–37.
6. Chen H, Jin Y, Chen H, Liao N, Wang Y, Chen J. MicroRNA-mediated inflammatory responses induced by *Cryptococcus neoformans* are dependent on the NF-κB pathway in human monocytes. Int J Mol Med. 2017;39(6):1525–32.
7. De Lacorte Singulani J, De Fátima Da Silva J, Gullo FP, Costa MC, Fusco-Almeida AM, Enguita FJ, et al. Preliminary evaluation of circulating microRNAs as potential biomarkers in paracoccidioidomycosis. Biomed Rep. 2017;6(3):353–7.
8. Kumar M, Ahmad T, Sharma A, Mabalirajan U, Kulshreshtha A, Agrawal A, et al. Let-7 microRNA-mediated regulation of IL-13 and allergic airway inflammation. J Allergy ClinImmunol. 2011;128(5):1077–85.
9. Essandoh K, Li Y, Huo J, Fan GC. miRNA-mediated macrophage polarization and its potential role in the regulation of inflammatory response. Shock. 2016;46(2):122–31.
10. Nahid MA, Yao B, Dominguez-Gutierrez PR, Kesavalu L, Satoh M, Chan EK. Regulation of TLR2-mediated tolerance and cross-tolerance through IRAK4 modulation by miR-132 and miR-212. J Immunol. 2013;190(3):1250–63.
11. Testa U, Pelosi E, Castelli G, Labbaye C. miR-146 and miR-155: two key modulators of immune response and tumor development. Noncoding RNA. 2017;3(3) :22.
12. Williamson PR. The relentless march of cryptococcal meningitis. Lancet Infect Dis. 2017;17:790–91.
13. Y. Li, X. Chen. miR-4792 inhibits epithelial-mesenchymal transition and invasion in nasopharyngeal carcinoma by targeting FOXC1. Biochemical and Biophysical Research Communications. 2015;468(4):863-869.
14. Georgieva B, Milev I, Minkov I, Dimitrova I, Bradford AP, Baev V. Characterization of the uterine leiomyoma microRNAome by deep sequencing. Genomics. 2012;99:275–281.
15. Chickooree D, Zhu K, Ram V, Wu HJ, He ZJ, Zhang S. A preliminary microarray assay of the miRNA expression signatures in buccal mucosa of oral submucous fibrosis patients. J. Oral Pathol. Med. 2016;45(9).
16. Gabrusiewicz K, Rodriguez B, Wei J, Hashimoto Y, Healy LM, Maiti SN, et al. Glioblastoma-infiltrated innate immune cells resemble M0 macrophage phenotype. JCI Insight. 2016;1(2):e85841.
17. Li CC, Eaton SA, Young PE, Lee M, Shuttleworth R, Humphreys DT, et al. Glioma microvesicles carry selectively packaged coding and non-coding RNAs which alter gene expression in recipient cells. RNA Biology. 2013;10:8:1333-1344.
18. Wang WY, Tan MS, Yu JT, Tan L. Role of pro-inflammatory cytokines released from microglia in Alzheimer's disease. Ann Transl Med. 2015; 3(10):136.
19. Jin X, Yamashita T. Microglia in central nervous system repair after injury. J Biochem. 2016;159:491–496.

20. Kraft AD, Harry GJ. Features of microglia and neuroinflammation relevant to environmental exposure and neurotoxicity. Int J Environ Res Public Health. 2011; 8:2980–3018.
21. O'Sullivan JB, Ryan KM, Curtin NM, Harkin A, Connor TJ. Noradrenaline reuptake inhibitors limit neuroinflammation in rat cortex following a systemic inflammatory challenge: implications for depression and neurodegeneration. Int J Neuropsychopharmacol. 2009;12:687–699.
22. Loane DJ, Byrnes KR: Role of microglia in neurotrauma. Neurotherapeutics. 2010;7:366–377.
23. Bachstetter AD, Xing B, de Almeida L, Dimayuga ER, Watterson DM, Van Eldik LJ. Microglial p38alpha MAPK is a key regulator of proinflammatory cytokine up-regulation induced by toll-like receptor (TLR) ligands or beta-amyloid (Abeta). J Neuroinflammation. 2011;8:79.
24. Xu L, Huang Y, Yu X, Yue J, Yang N, Zuo P. The influence of p38 mitogen-activated protein kinase inhibitor on synthesis of inflammatory cytokine tumor necrosis factor alpha in spinal cord of rats with chronic constriction injury. Anesth Analg. 2007;105:1838–1844.
25. Kim SH, Smith CJ, Van Eldik LJ. Importance of MAPK pathways for microglial pro-inflammatory cytokine IL-1 beta production. Neurobiol Aging. 2004;25:431–439.
26. Qu WS, Tian DS, Guo ZB, Fang J, Zhang Q, Yu ZY, et al. Inhibition of EGFR/MAPK signaling reduces microglial inflammatory response and the associated secondary damage in rats after spinal cord injury. Journal of Neuroinflammation. 2012;9:178.
27. Yamauchi T, Ueki K, Tobe K, Tamemoto H, Sekine N, Wada M, et al. Growth hormone-induced tyrosine phosphorylation of EGF receptor as an essential element leading to MAP kinase activation and gene expression. Endocr J. 1998;45:(Suppl):S27–S31.
28. Goel S, Hidalgo M, Perez-Soler R. EGFR inhibitor-mediated apoptosis in solid tumors. J Exp Ther Oncol. 2007;6(4).
29. Kwon-Chung KJ, Fraser JA, Doering TL, Wang Z, Janbon G, Idnurm A, et al. *Cryptococcus neoformans* and Cryptococcus gattii, the etiologic agents of cryptococcosis. Cold Spring Harb Perspect Med. 2014;4(7):a019760.
30. BIOSYNEX: Test CryptoPS. 2017; [cited 20 June 2017]
31. IMMY: CrAg LFA. 2017.
32. Martinez-Nunez RT, Louafi F, Sanchez-Elsner T. The interleukin 13 (IL-13) pathway in human macrophages is modulated by microRNA-155 via direct targeting of interleukin 13 receptor α1 (IL13Rα1). J Biol Chem. 2011;286(3):1786–94.
33. Roy S. miRNA in macrophage development and function. Antioxid Redox Signal. 2016;25(15):795–804.
34. Sabiiti W, Robertson E, Beale MA, Johnston SA, Brouwer AE, Loyse A, et al. Efficient phagocytosis and laccase activity affect the outcome of HIV-associated cryptococcosis. J Clin Invest. 2014;124:2000–2008.
35. Alanio A, Desnos-Ollivier M, Dromer F. Dynamics of *Cryptococcus neoformans*-macrophage interactions reveal that fungal background influences outcome during cryptococcal

meningoencephalitis in humans. MBio. 2011; 2(4).

36. Henn A, Lund S, Hedtjärn M, Schrattenholz A, Pörzgen P, Leist M. The suitability of BV2 cells as alternative model system for primary microglia cultures or for animal experiments examining brain inflammation. Altex. 2009;26:83–94.
37. Stansley B, Post J, Hensley K. A comparative review of cell culture systems for the study of microglial biology in Alzheimer's disease. J Neuroinflamm. 2012;9:577.
38. Kraft AD, Harry GJ. Features of microglia and neuroinflammation relevant to environmental exposure and neurotoxicity. Int J Environ Res Public Health. 2011;8:2980–3018.
39. 39. Julia Kofler, Clayton A.Wiley. Microglia: Key Innate Immune Cells of the Brain. Toxicologic Pathology, 2011;39:103-114.
40. R. Bryan Rock, Genya Gekker, Shuxian Hu, Wen S. Sheng, Maxim Cheeran, James R. Lokensgard, et al. Role of microglia in central nervous system infections. Clinical Microbiology Reviews. 2004;17(4):942–964.
41. Barluzzi R, Brozzetti A, Delfino D, Bistoni F, Blasi E. Role of the capsule in microglial cell-*Cryptococcus neoformans* interaction: Impairment of antifungal activity but not of secretory functions.Med. Mycol. 1998;36:189–197.
42. Neal LM, Xing E, Xu J, Kolbe JL, Osterholzer JJ, Segal BM, et al. CD4+T Cells Orchestrate Lethal Immune Pathology despite Fungal Clearance during *Cryptococcus neoformans* Meningoencephalitis. mBio. 2017;11,21;8(6).
43. Adami C, Sorci G, Blasi E, Agneletti AL, Bistoni F, Donato R. S100B expression in and effects on microglia. Glia. 2001;33:131–142.
44. Song X, Tanaka S, Cox D, Lee SC. Fc gamma receptor signaling in primary human microglia:Differential roles of PI-3K and Ras/ERK MAPK pathways in phagocytosis and chemokine induction.J. Leukoc. Biol. 2004;75:1147–1155.
45. Preissler J, Grosche A, Lede V, Le Duc D, Krügel K, Matyash V, et al. Altered Microglial Phagocytosis in GPR34-Deficient Mice. Glia. 2015;63:206–215.
46. Lee SC, Kress Y, Dickson DW, Casadevall A. Human Microglia Mediate Anti-*Cryptococcus neoformans* Activity in The Presence of Specific Antibody. J. Neuroimmunol. 1995;62:43–52.
47. Lee SC, Kress Y, Zhao ML, Dickson DW, Casadevall A. *Cryptococcus neoformans* survive and replicate in human microglia. Lab. Invest. 1995;73(6):871-879.
48. O'Sullivan JB, Ryan KM, Curtin NM, Harkin A, Connor TJ. Noradrenaline reuptake inhibitors limit neuroinflammation in rat cortex following a systemic inflammatory challenge: implications for depression and neurodegeneration. Int J Neuropsychopharmacol. 2009;12 :687–699.
49. Popovich PG, Guan Z, Wei P, Huitinga I, van Rooijen N, Stokes BT. Depletion of hematogenous macrophages promotes partial hindlimb recovery and neuroanatomical repair after experimental spinal cord injury. Exp Neurol. 1999;158:351–365.

50. Stirling DP, Khodarahmi K, Liu J, McPhail LT, McBride CB, Steeves JD, et al. Minocycline treatment reduces delayed oligodendrocyte death, attenuates axonal dieback, and improves functional outcome after spinal cord injury. J Neurosci. 2004;24:2182–2190.
51. Tian DS, Xie MJ, Yu ZY, Zhang Q, Wang YH, Chen B, et al. Cell cycle inhibition attenuates microglia induced inflammatory response and alleviates neuronal cell death after spinal cord injury in rats. Brain Res. 2007;1135:177–185.
52. Gomez-Pinilla F, Knauer DJ, Nieto-Sampedro M. Epidermal growth factor receptor immunoreactivity in rat brain. Development and cellular localization. Brain Res. 1988;438:385–390.
53. Erschbamer M, Pernold K, Olson L. Inhibiting epidermal growth factor receptor improves structural, locomotor, sensory, and bladder recovery from experimental spinal cord injury. J Neurosci. 2007;27:6428–6435.
54. Popovich PG, Guan Z, Wei P, Huitinga I, van Rooijen N, Stokes BT. Depletion of hematogenous macrophages promotes partial hindlimb recovery and neuroanatomical repair after experimental spinal cord injury. Exp Neurol. 1999;158:351–365.
55. Jung HW, Son HY, Minh CV, Kim YH, Park YK. Methanol extract of Ficus leaf inhibits the production of nitric oxide and proinflammatory cytokines in LPS-stimulated microglia via the MAPK pathway. Phytother Res. 2008;22:1064–1069.
56. Peigang liu, Jinbao Pu, Junhui Zhang, Zhilu chen, Kemin Wei, lian'gen shi. Bioinformatic analysis of mir-4792 regulates Radix Tetrastigma hemsleyani flavone to inhibit proliferation, invasion, and induce apoptosis of a549 cells. OncoTargets and Therapy. 2019;12:1401–1412.
57. Bocchini V, Mazzolla R, Barluzzi R, Blasi E, Sick P, Kettenmann H. An immortalized cell line expresses properties of activated microglial cells. J Neurosci Res. 1992;31:616–621.
58. Sheng W, Zong Y, Mohammad A, Ajit D, Cui J, Han D, et al. Pro-inflammatory cytokines and lipopolysaccharide induce changes in cell morphology, and upregulation of ERK1/2, iNOS and sPLA2-IIA expression in astrocytes and microglia. J Neuroinflammation. 2011;8:121.

Table

Table 1. List of primers for quantitative real-time PCR

	sequence
human GAPDH-F	5-*GCA*ℂ*GTC*∀*GGCTGAG*∀*C*-3
human GAPDH-R	5-*TGGTG*∀*GACG*ℂ*AGTGGA*-3
human EGFR-F	5-*G*ℂ∀*GGCACGAGT*∀*C*∀*GC*-3
human EGFR -R	5-*AGGGC*∀*TGAGGACAT*∀ℂ-3
mice GAPDH-F	5-*A*ℂ*CAG*∀*GACTGTGGATGG*-3
mice GAPDH-R	5-*TCTAGACGGCAGGTCAGGTC*-3
mice EGFR-F	5-*CTG*ℂ∀∀*G*⊤ℂ∀*GATGAGG*-3
mice EGFR-R	5-*GGGGCAC*⊤*C*⊤*CACACAGG*-3
miR-4792	CGGTGAGCGCTCGCTGGC

F, forward primer; R, reverse primer.

Figures

Figure 1

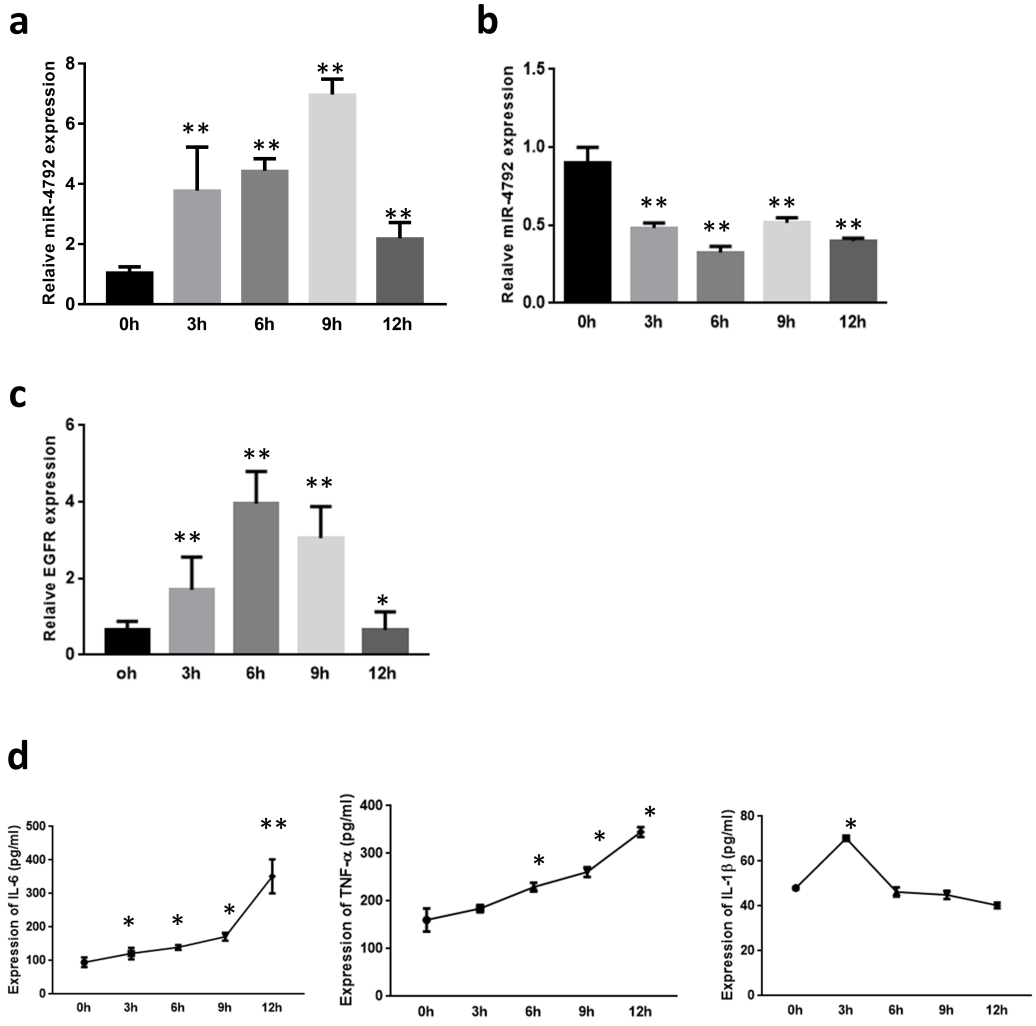

Figure 1

The expression of miR-4792 and EGFR in THP-1 cells and BV2 cells induced by Cryptococcus neoformans (WM148). (a) The levels of miR-4792 expression in THP-1 cells induced by WM148 at the indicated time points (0,3,6,9,12h) were determined by real-time PCR. Relative miRNAs levels are shown on the ordinate. Bars show means. The mean value in 0h was set at 1. (b) The levels of miR-4792 expression in BV2 cells induced by WM148 at the indicated time points (0,3,6,9,12h) were determined by

real-time PCR. Relative miRNAs levels are shown on the ordinate. Bars show means. The mean value in 0h was set at 1. (c) The levels of EGFR expression in BV2 cells induced by WM148 at the points in time (0,3,6,9,12h) were determined by real-time PCR. (d) Secretion of IL-6, TNF-α, and IL-1β was quantified by ELISA at the indicated time points. All results are expressed as mean ± SD from three independent experiments. *p< 0.05; **p < 0.01 compared with the control group.

Figure 2

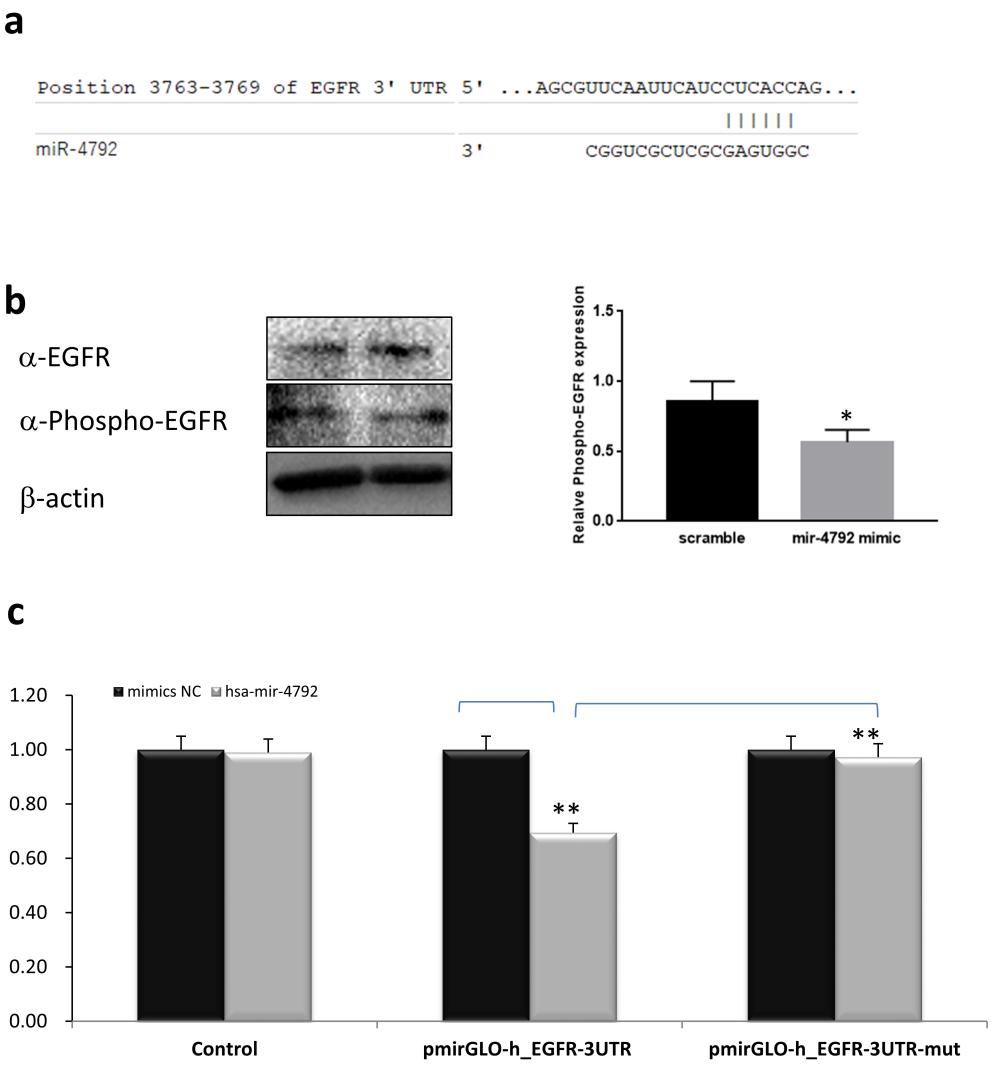

Figure 2

EGFR is a target gene of miR-4792. (a)Binding of miR-4792 with EGFR 3'-UTR was predicted by Targetscan. (b)Western blot was performed to detected the level of pEGFR in miR-4792 mimics group. p<0.05 compared with control group. β-actin served as the loading control. The protein levels of each molecule quantitated by scanning densitometry and corrected for the levels of β-actin in the same samples are shown on the ordinate. The maximum level in control was set at 1. Horizontal bars indicate average values. Vertical bars show SD. *p<0.05. **p<0.01. (c) Luciferase reporter assays were performed to verify the binding of miR-4792 in 3'-UTR of EGFR. *P<0.01 vs mimics NC.

Figure 3

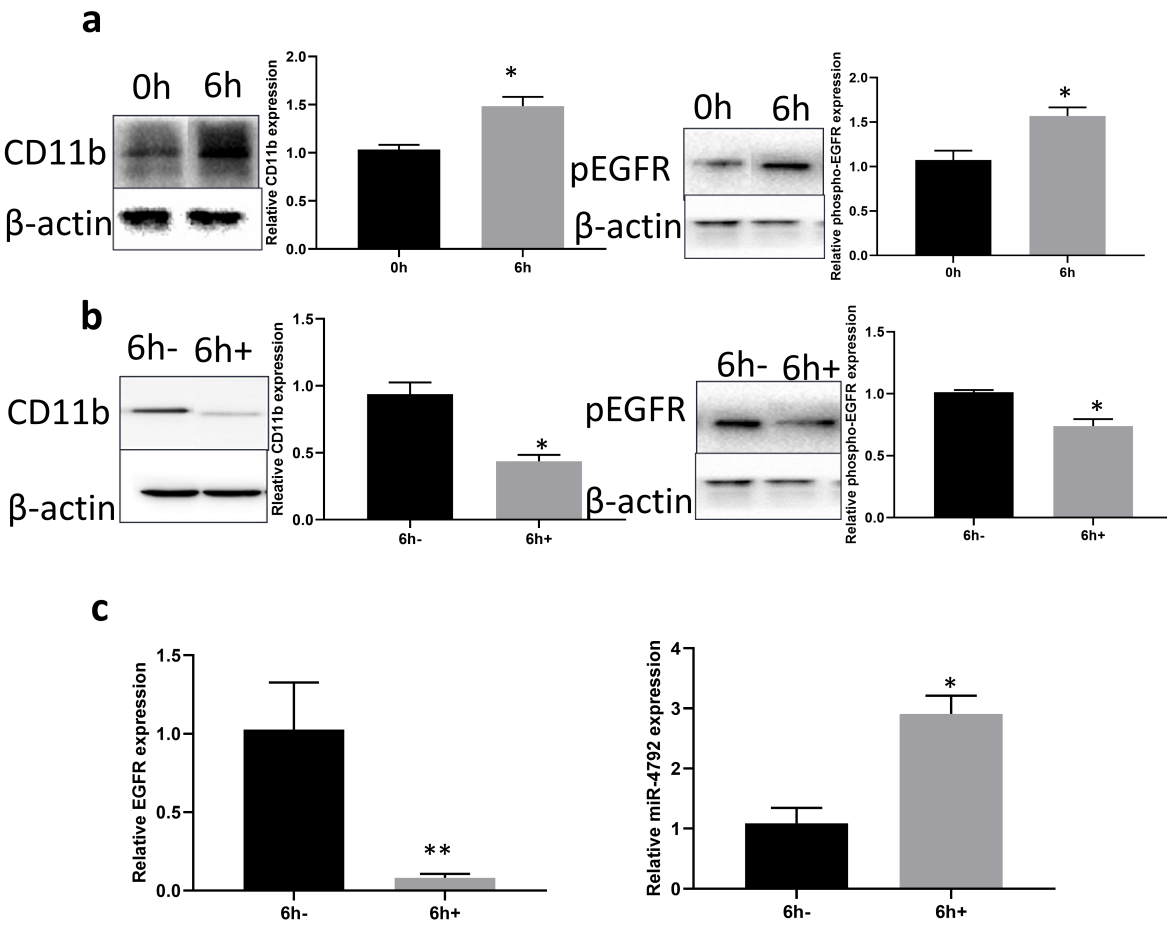

Figure 3

EGFR blockade inhibits WM148 induced microglia activation and EGFR phosphorylation and increased miR-4792 expression. Purified microglia was treated with WM148 for 6h before 40 μM AG1478 stimulation. (a) Western blot analysis of BV2 cells reveals that the WM148 induced upregulation of CD11b and pEGFR. $p<0.01$ vs control group. (b) Western blot demonstrates that AG1478 depressed CD11b and pEGFR in WM148 induced BV2 cells. $p<0.01$ vs only WM148 treated. (c) qRT-PCR reveals AG1478 significantly depressed EGFR expression while miR-4792 expression was increased. $p<0.01$ vs only WM148 treated. All results are expressed as mean ± SD from three independent experiments. *$p< 0.05$; **$p < 0.01$ compared with the control group.

Figure 4

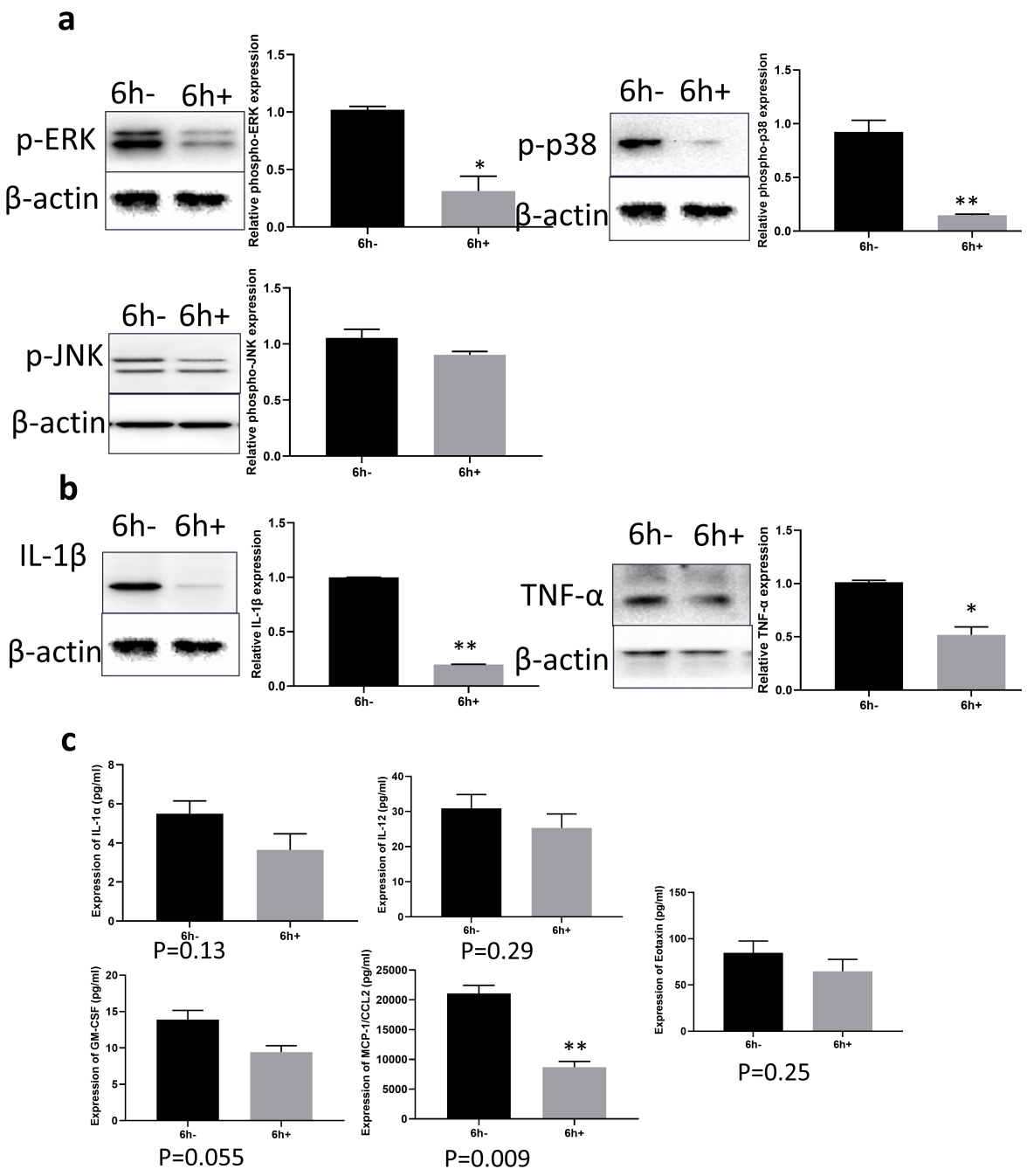

Figure 4

EGFR blockade depresses EGFR/MAPK activation and cytokine production. After treated with WM148 for 6h, 40 μM AG1478 was incubated for 24h. Western blot analysis of BV2 cells was performed to show phosphorylation of the MAPKs (ERK, JNK and p38) and cytokine production (IL-1β and TNFα). 6h-: only treated with WM148 for 6h; 6h+: After treated with WM148 for 6h, then incubated with 40 μM AG1478 for 24h. (a)p-ERK and p-p38 was significantly reduced by AG1478, while p-JNK was not significantly reduced

(*p<0.05,**p<0.01) (b)The expression of TNF-α, and IL-1β were significant depressed. *p< 0.05; **p < 0.01 vs only WM148 treated. (c) The expression of IL-1α, IL-12, Eotaxin, GM-CSF and MCP-1/CCL2 were depressed compared with the ones only WM148 treated. All results are expressed as mean ± SD from three independent experiments. *p< 0.05; **p < 0.01 compared with the control group.

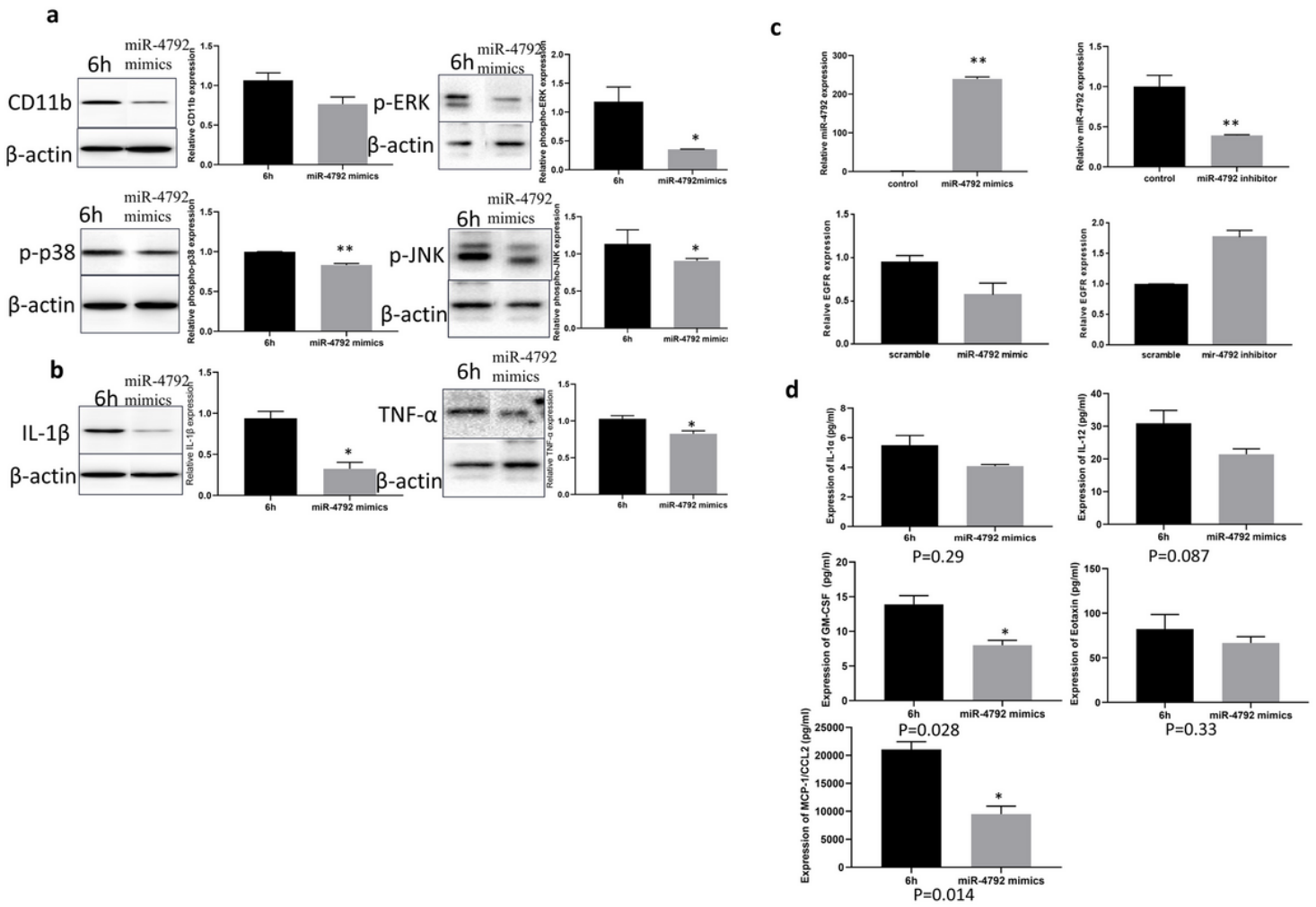

Figure 5

miR-4792 mimics depressed EGFR/MAPK activation and cytokine production. After treated with WM148 for 6h, 50 nM miR-4792 mimics was incubated for 24h. Western blot analysis of BV2 cells was performed to show phosphorylation of the MAPKs (ERK, JNK and p38) and cytokine production (IL-1β and TNFα). 6h: only treated with WM148 for 6h; miR-4792 mimics: After treated with WM148 for 6h, then incubated with 50 nM miR-4792 mimics for 24h. (a) Western blot analysis of BV2 cells reveals that miR-4792 mimics depressed CD11b and phosphorylation of the MAPKs (ERK, JNK and p38) in WM148 induced BV2 cells. p<0.05 vs only WM148 treated. (b) Western blot analysis of BV2 cells reveals that that miR-4792 mimics depressed the levels of the inflammatory cytokines IL-1β and TNFα significantly. p<0.05 vs only WM148 treated. (c)qRT-PCR showed miR-4792 was significantly increased/decreased by miR-4792 mimics/inhibitor, while the expression of EGFR was not statistically significant compared with control group. (d) Quantification of cytokines showed that miR-4792 mimics depressed the expression of IL-1α,

IL-12, Eotaxin, GM-CSF and MCP-1/CCL2 compared with the ones only WM148 treated. All results are expressed as mean ± SD from three independent experiments. *p< 0.05; **p < 0.01.

Figure 6

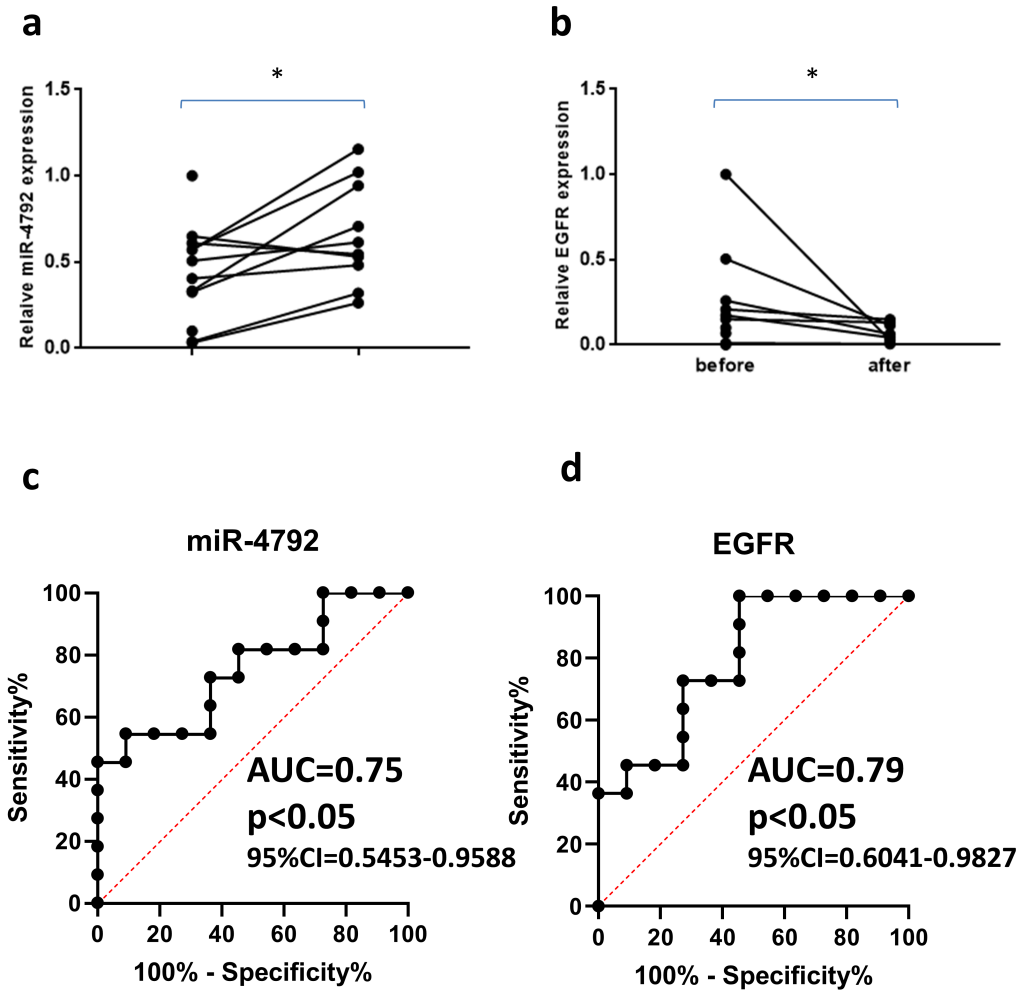

Figure 6

The expression of miR-4792 and EGFR in patients with cryptococcal meningitis before and after treatment. (a-b) qRT-PCR showed the expression of miR-4792 in CSF increased significantly after treatment, while the expression of EGFR in CSF decreased significantly after treatment. p<0.05. (c-d)

Receiver operating characteristic (ROC) curve for CSF miR-4792 and EGFR to distinguish patients with cryptococcal meningitis before and after treatment. AUC, areas under curves; CI, confidence interval. Data are means ± SD of three assays. *p< 0.05; **p < 0.01 compared with the control group.